Self-*Q*-switched waveguide laser based on femtosecond laser inscribed $Nd{:}Cr{:}YVO_4$ crystal

Yang Tan,[1,*,†] Yicun Yao,[1] John R. Macdonald,[2] Ajoy K. Kar,[2] Haohai Yu,[3] Huaijin Zhang,[3] and Feng Chen[1,4,†]

[1]*School of Physics, Key Laboratory of Particle Physics and Particle Irradiation, Ministry of Education, Shandong University, Jinan 250100, China*

[2]*Institute of Photonics and Quantum Sciences, Heriot–Watt University, Edinburgh EH14 4AS, UK*

[3]*State Key Laboratory of Crystal Materials, Shandong University, Jinan 250100, China*

[4]*e-mail: drfchen@sdu.edu.cn*

**Corresponding author: tanyang@sdu.edu.cn*

Received June 16, 2014; revised July 25, 2014; accepted July 28, 2014; posted July 30, 2014 (Doc. ID 214105); published September 4, 2014

We report on the self-*Q*-switched laser operation of a monolithic $Nd{:}Cr{:}YVO_4$ channel waveguide cavity. Femtosecond laser inscription was used to fabricate a buried channel waveguide in the substrate. The $Nd{:}Cr{:}YVO_4$ crystal works as both the gain medium and the saturable absorber, which enables the realization of a self-*Q*-switched waveguide laser pumped at 808 nm and emitting at 1064 nm. The compact waveguide cavity achieved maximum output powers up to 57 mW, corresponding to a single-pulse energy of 22.8 nJ, at 2.3 MHz repetition rate with a pulse duration of 85 ns.

OCIS codes: (230.7380) Waveguides, channeled; (130.3120) Integrated optics devices; (140.3540) Lasers, Q-switched.
http://dx.doi.org/10.1364/OL.39.005289

Materials with self-regulating features, such as self-frequency-doubling [1–3], self-Raman conversion [4,5], self-mode locking, and self-*Q*-switching [6–9], have attracted more and more attention because of their potential for compact, integrated devices. One of the most intriguing advantages over hybrid systems consisting of separated materials is that the optical devices based on self-regulating materials can be simplified, and typically have high stabilities. These features are particularly useful for the construction of integrated optical devices, usually with miniaturized spatial scales [10–14]. The realization of integrated devices relies on micromachining technologies, such as femtosecond laser inscription and ion irradiation [15–20]. For devices containing diverse materials, the manufacturing process is complicated, and additional losses will be unavoidable at the junctions of separate materials. Hence, materials with self-regulating functions are promising alternatives for the production of compact integrated devices.

Pulsed lasers have been applied in various fields, including nonlinear microscopy, frequency comb generation, and spectroscopy. Different from bulk lasers, waveguide lasers with compact geometries offer beam confinement on far smaller scales, providing an attractive light source for miniature photonic devices and on-chip integration [21–24]. Commonly, the *Q*-switched waveguide laser contains an extra section as the saturable absorber (SA) such as an organic dye, semiconductor SA or, in the case of Nd doped waveguides, chromium (Cr)-doped crystals placed between a resonator mirror and the end facet of the waveguide [25]. Among these absorbers, Cr ions doped crystals have the ability to be doped into a gain medium to form self-*Q*-switched laser devices.

Recently, it was reported that the neodymium (Nd) and Cr ion co-doped yttrium vanadate crystal ($Nd{:}Cr{:}YVO_4$) is a promising candidate for the generation of a self-*Q*-switched laser [26]. In the $Nd{:}Cr{:}YVO_4$ crystal, V^{5+} ions are substituted by Cr^{5+} ions without the balancing charge. Thus, the complexities in the crystal growth and problems in the applications could be avoided compared with Nd:Cr:YAG. Moreover, the $Nd{:}Cr{:}YVO_4$ crystal has a larger absorption and emission cross section, both desirable properties for a self-*Q*-switched laser material [26].

In this work, the $Nd{:}Cr{:}YVO_4$ crystal was used as the gain medium for the self-*Q*-switched waveguide laser. The waveguide structure in the crystal was fabricated by femtosecond laser inscription, which has been successfully applied for the waveguide laser fabrication in $Nd{:}YVO_4$ crystal [27]. Under the end-facet optical pumping, the pulse laser oscillation in the waveguides was observed and systematically investigated.

The sample used in this work was an $Nd{:}Cr{:}YVO_4$ single crystal grown by the Czochralski method under a nitrogen atmosphere containing 2% oxygen (v/v) in an iridium crucible. The Nd and Cr ion concentrations in the $Nd{:}Cr{:}YVO_4$ crystal were measured to be 0.79 and 1.40 at. %, respectively. The crystal was cut into pieces with the dimension of $7\ \mathrm{mm} \times 5\ \mathrm{mm} \times 2\ \mathrm{mm}$ ($a \times b \times c$) and optically polished. The channel waveguide was fabricated by femtosecond laser inscription using the "Type II" or "double-line" structure [18] in the crystal with a similar design to those previously demonstrated in the $Nd{:}YVO_4$ [27]. The inscription laser used was an IMRA-Jewel D400 ultrafast fiber laser system that emitted a 200 kHz train of 350 fs (FWHM) pulses at a central wavelength of 1047 nm. The pulses were focused approximately 100 μm below the sample surface using an aspheric lens with a numerical aperture (NA) of 0.6. The average laser beam power on the sample was set to 140 mW corresponding to a pulse energy of 700 nJ. The two parallel damage tracks that form Type II waveguides were inscribed along the "a" axis with a separation of 20 μm, which has a length of 7 mm. In addition, the sample was translated through the fabrication beam at a velocity of 17 mm/s. The translation direction used to inscribe both tracks was the same.

The polarization dependent emission spectra of the $Nd{:}Cr{:}YVO_4$ waveguide was measured at room temperature with the pumping wavelength at 810 nm. During the experiment, the pumping laser, with the polarization perpendicular to the a axis and c axis, was coupled into the waveguide structure. The output light was collected and focused onto a spectrometer with the measurement error of approximately 2 nm.

Figure 1 shows the experimental setup for the waveguide laser cavity. A continuous wave (cw) Ti: sapphire laser (Coherent MBR 110) was used as the pump laser and coupled into the waveguide through a specially designed convex lens ($f = 25$ mm). The pump laser allowed wavelengths across the crystal absorption bandwidth to be investigated, in this case 800–830 nm. A long working distance microscope objective (20×, NA = 0.4) was used to collect the output light from the opposite facet. As no laser mirrors were used in this experiment, Fresnel reflections of 8.6% at the end facets were used as the output coupler which was calculated to be 99%. The laser cavity described below therefore has a robust monolithic cavity architecture suited to applications outside of the laboratory. Further improvement to the cavity design could be realized through a dichroic coating on the pump input facet of the waveguide providing high reflectivity for the signal wavelength.

Figure 2(a) shows the cross section of the waveguide structure, which has a separation distance of 20 μm between the two inscribed elements. Two regions of damage can be seen to have been affected by the laser inscription process, in which the refractive index was decreased. This modification in turn results in an increase of refractive index induced in the region between the two inscribed elements because of the strain-optic effect. Through the combination of the increase and decrease of the refractive index, the waveguide structure was formed between the two inscribed "tracks." Light with both π and σ polarizations could be confined in the waveguide structure, both showing comparable mode-field profiles. Figures 2(b) and 2(c) depict the propagating mode for π polarization at the wavelengths of 808 and 1064 nm, respectively. Single mode propagation was observed at both wavelengths, which importantly provides strong mode overlap between the pump and emission signals. Characterization of the structures was performed with both π and σ polarizations at a wavelength of 1064 nm. The propagation loss of the waveguide was measured to be 1.4 and 1 dB/cm^{-1}, respectively. As the luminescence of Nd:Cr:YVO_4 is strongly polarization dependent with a larger emission cross section for π polarization, we focused the discussion on the laser oscillation with pump light of the π polarization direction in this Letter.

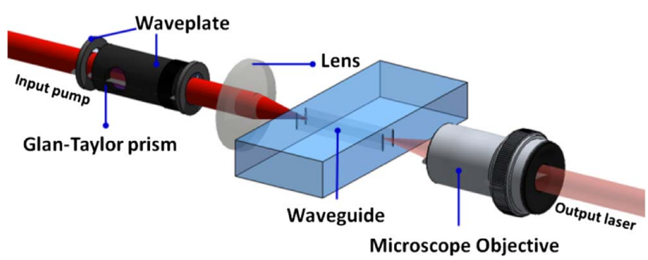

Fig. 1. Experiment setup for the self-Q-switched waveguide laser generation.

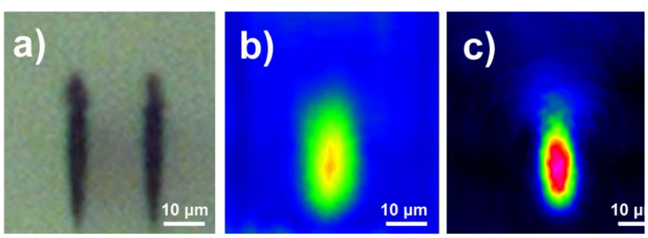

Fig. 2. (a) Cross sectional microscope image of the inscribed Type II waveguide in the Nd:Cr:YVO_4 crystal; the measured modal profile of (b) the pumping laser at 808 nm and (c) the output laser at ~1064 nm.

Figure 3 depicts the luminescence spectra obtained from the waveguide and unmodified bulk at the room temperature. Pumped by a laser at 808 nm with π polarization, emission peaks around 900, 1064, and 1310 nm were observed, among which the emission peak at 1064 nm has the strongest relative intensity. Compared with the waveguide and the bulk, shapes and position of fluorescence peaks were similar to each other. This indicates that the fluorescence property of the material in the waveguide was preserved during the femtosecond laser inscription process.

Increasing the power of the pump laser, laser oscillation was observed in the waveguide structure. Figure 4 shows the emission spectra of the laser output from the Nd:Cr:YVO_4 channel waveguide at room temperature, in which a peak with the full width at half-maximum (FWHM) 2 nm was observed centered at the wavelength of 1064 nm. With the pump power of 208 mW along π polarization, the output power of the laser was measured with the variation of the pump wavelength from 800 to 830 nm. As shown in Fig. 4(b), the Nd:Cr:YVO_4 waveguide has a broad absorption bandwidth. There were two strong absorption peaks centered at 808 and 815 nm with FWHM of 6 nm and the value of the output power were 57 and 54 mW, respectively. With the wavelength tuning to 800 and 830 nm, the value of the output power was decreased to zero. The width of the absorption line was broader, which may be induced by the variation in the

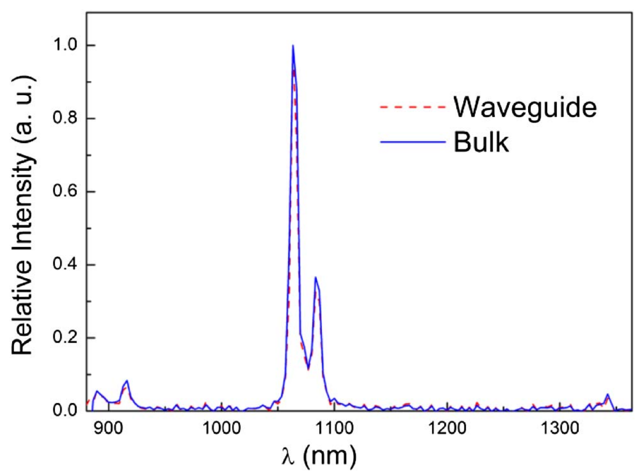

Fig. 3. Room-temperature luminescence spectra obtained from the waveguide (red-dashed line) and bulk (blue solid line) at the room temperature pumped by the laser at the wavelength of 808 nm.

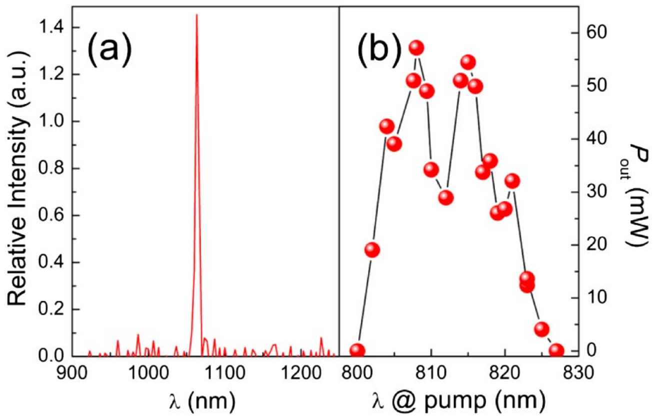

Fig. 4. (a) Laser oscillation spectra of the self-Q-switched waveguide laser. (b) Maximum power of the output laser as a function of the wavelength of the pumping laser with π polarization.

crystal field, in which there was a random distribution of Cr and V ions at the V-ion sites. In addition, the direct diode pump of the Nd:Cr:YVO_4 waveguide system is feasible because of the broad bandwidth of the absorption line.

Figure 5 shows the laser output power at 1064 nm as a function of the absorbed pump power at 808 nm in the waveguide structure. The pump power at the threshold of emission was 50 mW. When the pump power exceeded 120 mW, typical Q-switched pulse trains were observed. As depicted in the inset of Fig. 5, the pulse duration of the self-Q-switched pulses was 85 ns. At an average output power of 42 mW, the corresponding Q-switched repetition was 1.85 MHz and therefore the pulse energy obtained was 23 nJ.

As the pumping power was increased, an increase in the pulse repetition rate was observed (see Fig. 6). At a pump power of 114 mW, the repetition rate of the Q-switched pulse laser was 0.78 MHz. Upon increasing the pump power to 208 mW, the repetition rate was observed to increase to 2.3 MHz. A clear linear relationship between the repetition rate and pump power can be seen in Fig. 6. Furthermore, the duration of the pulse remained stable at 85 ns with a variation of the pump power, which is indicative of stable Q-switched operation.

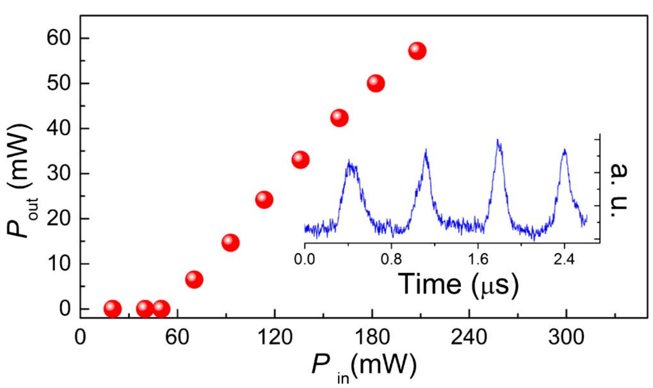

Fig. 5. Output power of 1064 nm laser as a function of the absorbed pumping power at 808 nm. The pulse train of pulsed laser is shown in the inset with the pumping power of 160 mW.

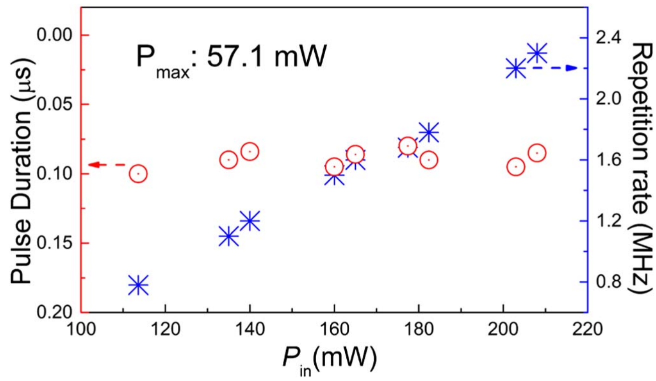

Fig. 6. Variation of the pulse duration and the repetition rate of the self-Q-switched pulse waveguide laser as a function of the input pumping power.

In summary, a pulsed operation channel waveguide laser was realized through self-Q-switching process in Nd:Cr:YVO_4. Type II double-line waveguide structures were successfully fabricated by femtosecond laser inscription and demonstrated propagation losses as low as 1 dB/cm^{-1}. The waveguides were used as a monolithic laser cavity, producing self-Q-switched output with a pulse duration of 85 ns, a maximum average power of 57 mW, at a repetition rate of 2.3 MHz. Furthermore, the compact, robust, and vibration insensitive nature of the monolithic waveguide cavity is well suited to real world applications.

This work was supported by National Natural Science Foundation of China (No. 11274203), the 111 Project (No. B13029), and Fundamental Research Funds for Shandong University (No. 2014JC002).

†These authors contributed equally to this work.

References

1. Y. Tan, Q. Luan, F. Chen, D. Jaque, and J. R. V. de Aldana, Phys. Status Solidi RRL **7**, 1018 (2013).
2. H. H. Yu, H. J. Zhang, Y. C. Wang, Z. P. Wang, J. Y. Wang, and V. Petrov, Sci. Rep. **3**, 1085 (2013).
3. D. Jaque, J. Capmany, F. Molero, and J. G. Sole, Appl. Phys. Lett. **73**, 3659 (1998).
4. R. Li, R. Bauer, and W. Lubeigt, Opt. Express **21**, 17745 (2013).
5. Y. Lü, X. Zhang, S. Li, J. Xia, W. Cheng, and Z. Xiong, Opt. Lett. **35**, 2964 (2010).
6. J. Dong, P. Deng, Y. Lu, Y. Zhang, Y. Liu, J. Xu, and W. Chen, Opt. Lett. **25**, 1101 (2000).
7. H. H. Yu, H. J. Zhang, Z. P. Wang, J. Y. Wang, Y. G. Yu, W. L. Gao, X. T. Tao, and M. H. Jiang, Opt. Express **16**, 3320 (2008).
8. M. Nakazawa, K. Suzuki, H. Kubota, and Y. Kimura, Opt. Lett. **18**, 613 (1993).
9. Z. J. Chen, A. B. Grudinin, J. Porta, and J. D. Minelly, Opt. Lett. **23**, 454 (1998).
10. Y. Ren, Y. Jia, F. Chen, Q. Lu, Sh. Akhmadaliev, and Sh. Zhou, Opt. Express **19**, 12490 (2011).
11. Y. Jia, F. Chen, J. R. V. de Aldana, Sh. Akhmadaliev, and Sh. Zhou, Opt. Mater. **34**, 1913 (2012).
12. J. Kim, S. Choi, D. Yeom, Sh. Aravazhi, M. Pollnau, U. Griebner, V. Petrov, and F. Rotermund, Opt. Lett. **38**, 5090 (2013).
13. C. Zhao, Y. Zou, Y. Chen, Z. Wang, S. Lu, H. Zhang, S. Wen, and D. Tang, Opt. Express **20**, 27888 (2012).

14. Y. Chen, C. Zhao, H. Huang, S. Chen, P. Tang, Z. Wang, S. Lu, H. Zhang, S. Wen, and D. Tang, IEEE J. Lightwave Technol. **31**, 2857 (2013).
15. J. Siebenmorgen, T. Calmano, K. Petermann, and G. Huber, Opt. Express **18**, 16035 (2010).
16. T. Calmano, A. Paschke, S. Müller, C. Kränkel, and G. Huber, Opt. Express **21**, 25501 (2013).
17. S. Müller, T. Calmano, P. W. Metz, C. Kränkel, C. Canalias, C. Liljestrand, F. Laurell, and G. Huber, Opt. Lett. **39**, 1274 (2014).
18. F. Chen and J. R. V. de Aldana, Laser Photon. Rev. **8**, 251 (2014).
19. F. Chen, Laser Photon. Rev. **6**, 622 (2012).
20. D. Choudhury, J. R. Macdonald, and A. K. Kar, Laser Photon. Rev., doi: 10.1002/lpor.201300195 (2014).
21. F. M. Bain, A. A. Lagatsky, S. V. Kurilchick, V. E. Kisel, S. A. Guretsky, A. M. Luginets, N. A. Kalanda, I. M. Kolesova, N. V. Kuleshov, W. Sibbett, and C. T. A. Brown, Opt. Express **17**, 1666 (2009).
22. J. I. Mackenzie and D. P. Shepherd, Opt. Lett. **27**, 2161 (2002).
23. W. Bolaños, J. J. Carvajal, X. Mateos, E. Cantelar, G. Lifante, U. Griebner, V. Petrov, V. L. Panyutin, G. S. Murugan, J. S. Wilkinson, M. Aguilo, and F. Díaz, Opt. Express **19**, 1449 (2011).
24. Y. Jia, F. Chen, and J. R. V. de Aldana, Opt. Express **20**, 16801 (2012).
25. T. Calmano, A. Paschke, S. Mueller, C. Kraenkel, and G. Huber, in *Lasers, Sources, and Related Photonic Devices*, OSA Technical Digest (CD) (Optical Society of America, 2012), paper IF2A.4.
26. Z. B. Pan, B. Yao, H. H. Yu, H. H. Xu, Z. P. Wang, J. Y. Wang, and H. J. Zhang, Opt. Express **20**, 2178 (2012).
27. Y. Tan, F. Chen, J. R. V. de Aldana, G. A. Torchia, A. Benayas, and D. Jaque, Appl. Phys. Lett. **97**, 031119 (2010).